

# Overfitting in quantum machine learning and entangling dropout

Masahiro Kobayashi<sup>1</sup> · Kohei Nakaji<sup>2,3</sup> · Naoki Yamamoto<sup>1,2</sup>

the date of receipt and acceptance should be inserted later

**Abstract** The ultimate goal in machine learning is to construct a model function that has a generalization capability for unseen dataset, based on given training dataset. If the model function has too much expressibility power, then it may overfit to the training data and as a result lose the generalization capability. To avoid such overfitting issue, several techniques have been developed in the classical machine learning regime, and the dropout is one such effective method. This paper proposes a straightforward analogue of this technique in the quantum machine learning regime, the entangling dropout, meaning that some entangling gates in a given parametrized quantum circuit are randomly removed during the training process to reduce the expressibility of the circuit. Some simple case studies are given to show that this technique actually suppresses the overfitting.

## 1 Introduction

Quantum computer has potential to execute machine learning tasks more efficiently than conventional computers [1–3]. Both in classical and quantum machine learning problems, it is important to use an approximator (a model function) that has a high expressibility power to achieve a good computational accuracy. For this purpose, recently the data re-uploading method was proposed [4–6], which encodes the input data into the quantum circuit multiple times in the depth direction of the circuit. On the other hand, if the expressibility is too high, then the approximator may overfit to the training dataset and lose the generalization capability for

unseen dataset. That is, we need to carefully design an approximator with appropriate expressibility power, such that it can achieve as small generalization (out-of-sample) error as possible. In fact, we recently find some theoretical analysis on the generalization error in quantum machine learning regime [7–12], although practical quantum-oriented methods for suppressing the overfitting issue have not been sufficiently discussed.

In this paper, we propose a practical method for suppressing the overfitting issue in quantum machine learning problems, the *entangling dropout*. This is a straightforward analogue of the classical dropout [13], which randomly removes some connections between nodes of a neural network during the training process; although the mechanism for suppressing the overfitting has not been fully revealed, the effectiveness of classical dropout is very well recognized, and it has been widely used. The proposed entangling dropout employs a similar technique, that randomly removes some entangling gates contained in a given parametrized quantum circuit during the training process. This clearly decreases the expressibility, but how to choose the dropout ratio, which determines the number of entangling gates removed in each iteration, is not trivial for suppressing the overfitting and achieving the target performance. We show a detailed case study of this problem. Also a comparison to the standard  $L_1$  or  $L_2$  regularization technique is provided, showing a merit of using the entangling dropout method.

Note that recently another type of dropout for quantum machine learning was proposed [14, 15]; this scheme randomly removes a qubit, by directly measuring it and discarding the result (i.e., taking the partial trace) followed by adding another qubit to the same place. Hence this scheme may be termed the qubit dropout. Clearly this operation completely blocks the information flow on the quantum circuit, reflecting a more straightforward analogue to the classical dropout. On the other hand, the entangling dropout is eas-

1, Department of Applied Physics and Physico-Informatics, Keio University, Hiyoshi 3-14-1, Kohoku, Yokohama 223- 8522, Japan

2, Quantum computing center, Keio University, Hiyoshi 3-14-1, Kohoku, Yokohama 223- 8522, Japan

3, Present address: Research Center for Emerging Computing Technologies, National Institute of Advanced Industrial Science and Technology (AIST), 1-1-1 Umezono, Tsukuba, Ibaraki 305-8568, Japan

ier to implement, compared to the qubit dropout that needs an intermediate measurement on a circuit. Comparing the effect of these two type of regularization methods is interesting, but in this paper we only investigate the proposed entangling dropout.

## 2 Overfitting in quantum machine learning

### 2.1 The quantum circuit model

We use the following  $n$ -qubits quantum circuit to construct an approximator; for an input vector  $x$ , the scalar-valued output is given by

$$f_L(x; \theta) = \langle 0^n | U_L^\dagger(x; \theta) A U_L(x; \theta) | 0^n \rangle, \quad (1)$$

$$U_L(x; \theta) = W(\theta^{(L)}) S(x) W(\theta^{(L-1)}) S(x) \cdots W(\theta^{(1)}) S(x),$$

where  $A$  is an observable and  $|0^n\rangle = |0\rangle^{\otimes n}$  with  $|0\rangle$  the computational 0 state.  $W(\cdot)$  is the unitary matrix representing a parametrized quantum circuit, where  $\theta = (\theta^{(1)}, \dots, \theta^{(L)})$  is the set of tunable parameters with  $\theta^{(\ell)}$  the vector of parameters contained in the  $\ell$ th  $W(\cdot)$ .  $S(x)$  is a circuit for encoding  $x$ , which is composed of the unitaries of the form  $e^{-ig(x)H}$  in the 1-dimensional case  $x \in \mathbb{R}$  with  $g(x) \in \mathbb{R}$  a function we can arbitrarily choose. It is then shown in Ref. [6] that  $f_L(x; \theta)$  can be expressed as the following Fourier form

$$f_L(x; \theta) = \sum_{\omega \in \Omega} c_\omega(\theta) e^{i\omega g(x)},$$

where  $\Omega$  denotes the discrete set of frequencies. The number of elements of  $\Omega$  is an increasing function of  $L$ , implying the importance of multiple use of the encoder  $S(x)$  for the purpose of enhancing the expressibility power of  $f_L(x; \theta)$ .

### 2.2 Example of overfitting

Let us consider a simple 1-dimensional regression problem; given a training dataset  $\{(x_k, y_k)\}_{k=1, \dots, D}$  with  $x_k \in \mathbb{R}$ , the task is to determine  $\theta$  so that the cost (in-sample error)

$$J_r(\theta) = \frac{1}{D} \sum_{k=1}^D (y_k - f_L(x_k; \theta))^2 \quad (2)$$

is minimized. Here we take a  $n = 5$  qubit model, with the encoding circuit  $S(x)$  and the tuning circuit  $W(\cdot)$  illustrated in Fig. 1; note that  $S(x)$  is composed of  $R_y(\sin^{-1}x)$  etc., rather than  $R_y(x)$ , to enhance the nonlinearity of the function. The output is defined through  $A = Z_1 = Z \otimes I^{\otimes 4}$  with  $Z$  the Pauli- $Z$  matrix and  $I$  the  $2 \times 2$  identity matrix.

Recall now that the final goal of machine learning is to construct an approximator that has a good generalization capability, i.e., the function having a small out-of-sample error

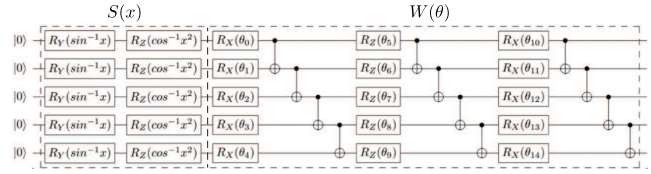


**Fig. 1** Diagram of the encoding circuit  $S(x)$  and the tuning circuit  $W(\theta)$  in the case  $n = 5$ .

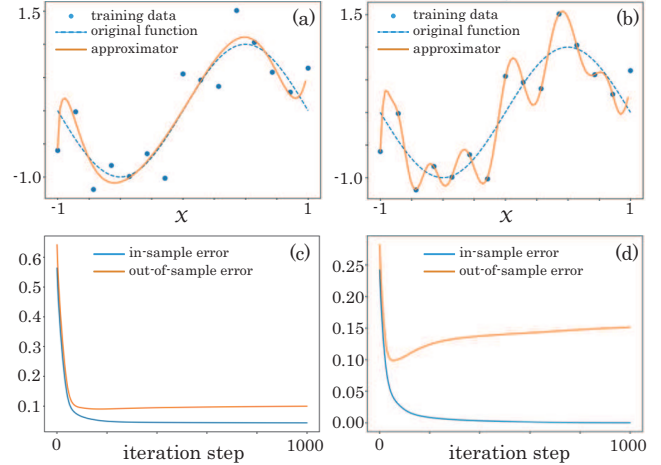


**Fig. 2** (a, b) Training dataset (blue points) and the generated approximator  $f_1(x; \theta)$  for (a) and  $f_{10}(x; \theta)$  for (b). (c, d) In-sample (training) error and out-of-sample (test) error achieved by  $f_1(x; \theta)$  for (c) and  $f_{10}(x; \theta)$  for (d).

for unseen dataset (or test dataset):

$$J'_r(\theta) = \frac{1}{D'} \sum_{k=1}^{D'} (y'_k - f_L(x'_k; \theta))^2,$$

where  $\{(x'_k, y'_k)\}_{k=1, \dots, D'}$  is the test dataset; note that  $J'_r(\theta)$  is not used to train  $\theta$ . If the approximator  $f_L(x; \theta)$  has too much expressibility, then  $J'_r(\theta)$  can take a large value even when  $J_r(\theta)$  is well suppressed, i.e., overfitting to the training dataset. This issue can actually be seen in the case where the training dataset is generated from  $y = \sin(\pi x)$  with Gaussian noise; the dataset and  $y = \sin(\pi x)$  are illustrated by the blue points and the blue dotted-line, respectively, in Fig. 2 (a), (b). We apply two models  $f_1(x; \theta)$  and  $f_{10}(x; \theta)$ ; as  $n = 5$ , the number of parameters of these models are 15 and 150, respectively. Clearly,  $f_{10}(x; \theta)$  contains more frequency components (i.e., the size of  $\Omega$  is bigger) and accordingly has bigger expressibility than  $f_1(x; \theta)$ . After 1000 times update of parameters (we used Adam),  $f_{10}(x; \theta)$  overfits to the training dataset while  $f_1(x; \theta)$  looks a modest approximator, as shown in Fig. 2 (a), (b).

The overfitting issue can also be seen in the training process; Fig. 2 (c) shows the in-sample error  $J_r(\theta_j)$  and the out-of-sample error  $J'_r(\theta_j)$  at the iteration step  $j$ , in the case (c)  $L = 1$  and the case (d)  $L = 10$ . Note that  $J'_r(\theta_j)$  is computed with the learned parameter  $\theta_j$  obtained using  $J_r(\theta)$ .

Clearly, as  $J_r(\theta_j)$  decreases, or equivalently the model becomes a better approximator to the training dataset,  $J'_r(\theta_j)$  for the case  $L = 10$  increases after at about  $j = 200$  iteration steps, while that of  $L = 1$  becomes almost constant. This is a well recognized phenomenon of overfitting that the out-of-sample error increases after some point of the parameter update, implying the necessity of early-stopping of the training which is also often used as a regularization technique for avoiding overfitting.

Lastly note that there have been some discussion stating that overfitting may not occur for the case  $L = 1$  [2, 10], which is actually consistent to the above numerical simulation result.

### 3 Entangling dropout

#### 3.1 Method

The expressibility of a parameterized quantum circuit heavily depends on the number of entangling gates over qubits. Hence, similar to the dropout method for neural networks, we propose a method to reduce the expressibility by randomly removing some entangling gates contained in the circuit during the training process – entangling dropout. A more precise description of the method is as follows:

1. Remove some entangling gates randomly at the  $j$ th iteration step of parameters.
2. Calculate the gradient of the cost function, for the circuit with dropout executed, to determine the  $(j + 1)$ th parameters using the gradient descent method.
3. Repeat the above procedure until a desired performance is reached.

Note that the entangling dropout is executed independently at each iteration step, as in the classical case; hence, the average number of entangling gates is constant through the whole learning process. The random removal is determined by the following rule:

1. Randomly choose layers in which some entangling gates are to be removed. The probability of choosing a layer to which the dropout is applied is called the *layer dropout ratio*.
2. Then randomly remove entangling gates in the chosen layers. The probability of removing an entangling gate is called the *gate dropout ratio*.

For instance, let us consider the circuit with  $n = 5$  and  $L = 10$ , and the case where the layer dropout rate and the gate dropout ratio are 0.2 and 0.3, respectively. In this case, on average,  $10 \times 0.2 = 2$  layers are first chosen randomly and then  $12 \times 0.3 = 3.6$  entangling gates in each chosen layer are randomly removed; Fig. 3 shows the case where 3 CNOT gates are removed. These two hyper parameters should be carefully designed.

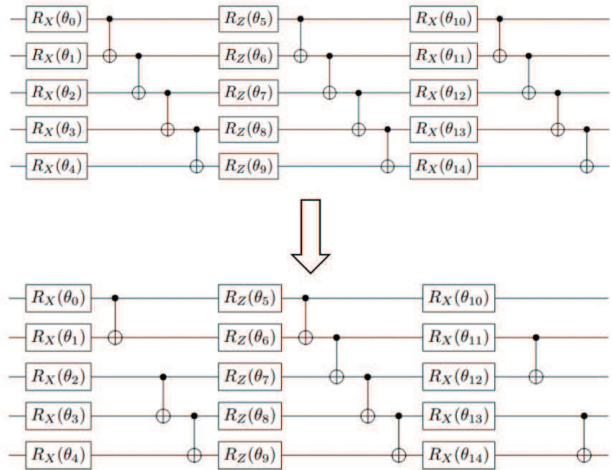


**Fig. 3** Example of removing CNOT gates with gate dropout rate 0.3, for the chosen layer  $W(\cdot)$ .

#### 3.2 Suppression of overfitting

Here we demonstrate the performance of entangling dropout method. We continue to study the same regression problem discussed in Section 2.2, where both the training and test datasets are generated from  $y = \sin(\pi x)$  with Gaussian noise; also the same circuit of  $n = 5$  qubits and  $L = 10$  layers is taken. The approximator  $f_{10}(x; \theta)$  constructed through the learning process is illustrated in Fig. 4 (a), which is the same as Fig. 2 (b); as seen before, because this approximator contains too many frequency components and accordingly have too much expressibility, overfitting occurs. Also recall the orange line in Fig. 2 (d) showing that the out-of-sample error increases, which is the same as the blue line in Fig. 4 (c). Now we apply the entangling dropout with layer dropout rate 0.2 and gate dropout rate 0.2, to this circuit. Because the dropout is a stochastic operation, the constructed approximator differs in every trial; one example is illustrated in Fig. 4 (b), showing that the approximator with dropout does not overfit to the training dataset, compared to that without dropout. As a result, the out-of-sample error does not increase, as illustrated in Fig. 4 (c) showing the mean, standard deviation, and the minimum envelope of 5 sample paths of out-of-sample errors.

To support the above observation emphasizing the usefulness of entangling dropout, we show another example of regression problem; the function generating the training and test dataset is  $y = |x| - 1/2$ . The circuit is exactly the same as the previous case. The layer and gate dropout rate are 0.2 and 0.5. The result is summarized in Fig. 5, which may lead to the same conclusion reached above; that is, the dropout is effectively used for suppressing the overfitting and consequently the out-of-sample error does not increase.

It is also worth studying the effect of entangling dropout for a classification problem. Here we study the following

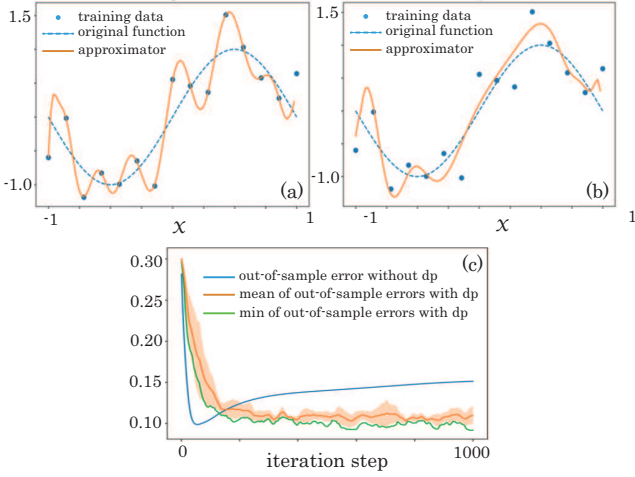


**Fig. 4** (a, b) Training dataset (blue points) generated from  $y = \sin(\pi x)$  with Gaussian noise (blue dotted line), and the constructed approximator  $f_{10}(x; \theta)$  without dropout (a) and with dropout (b). (c) Out-of-sample (test) errors achieved by  $f_{10}(x; \theta)$  without dropout (blue solid line) and with dropout (mean: red solid line, min: green solid line). The orange shade represents the standard deviation of 5 learning curves, fluctuating with respect to the randomness in dropout.

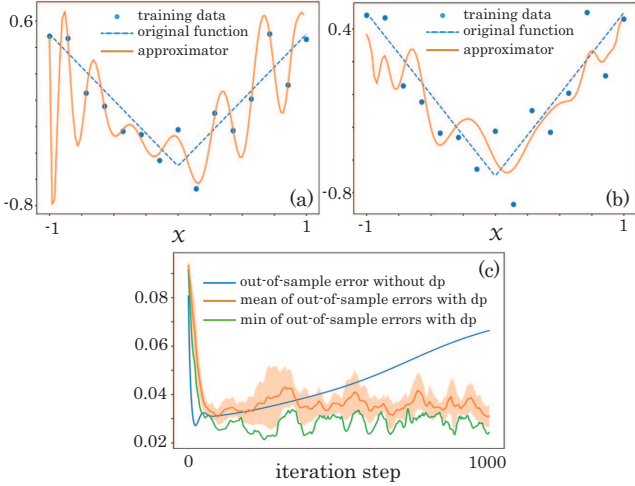


**Fig. 5** (a, b) Training dataset (blue points) generated from  $y = |x| - 1/2$  with Gaussian noise (blue dotted line), and the constructed approximator  $f_{10}(x; \theta)$  without dropout (a) and with dropout (b). (c) Out-of-sample (test) errors achieved by  $f_{10}(x; \theta)$  without dropout (blue solid line) and with dropout (mean: red solid line, min: green solid line). The orange shade represents the standard deviation of 5 learning curves, fluctuating with respect to the randomness in dropout.

2-dimensional 2-label classification problem; given a training dataset  $\{(x_k, y_k)\}_{k=1, \dots, D}$  where the vector  $y_k = (1, 0)$  or  $(0, 1)$  represents the class assigned to the input  $x_k \in \mathbb{R}^2$ , the task is to construct a probabilistic classifier that assigns the label based on the probability vector

$$F(x) = \frac{1}{e^{z_1} + e^{z_2}} \begin{bmatrix} e^{z_1} \\ e^{z_2} \end{bmatrix} = \begin{bmatrix} 1/(1 + e^{-f_L(x; \theta)}) \\ 1/(1 + e^{f_L(x; \theta)}) \end{bmatrix}.$$

Here  $f_L(x; \theta)$  is given in Eq. (1) with  $A = (Z \otimes I - I \otimes Z) \otimes I^{\otimes (n-2)}$ . The parameters  $\theta$  are determined so that the cross

entropy cost (in-sample error)

$$J_c(\theta) = \sum_{k=1}^D y_k^\top \log F(x_k)$$

is minimized (log is taken elementwise). We again consider the case  $n = 5$  and the same circuits  $S(x)$  and  $W(\theta)$  illustrated in Fig. 1, with  $L = 10$ . Then we compare the classifiers with and without entangling dropout; the layer and gate dropout rate are 0.2 and 0.3. The two-class training dataset is illustrated by the blue and red points in Fig. 6 (a), (b). The constructed classifier is depicted as the boundary dividing the blue and red regions in Fig. 6, where (a) and (b) represent the case without and with dropout, respectively. Though not so visible, the classifier without dropout (a) looks like separating two regions with more complicated boundaries, compared to that with dropout (b). Figure 6 (c) shows the out-of-sample errors over the training process of the classifier with and without dropout; recall that the dropout is a stochastic operation, and here the mean, standard deviation, and the minimum envelope of 5 sample paths of out-of-sample errors with dropout are shown. As in the regression case, the out-of-sample error without dropout increases after about 700 iteration steps, reflecting the overfitting, while the out-of-sample error with dropout does not show such a trend.

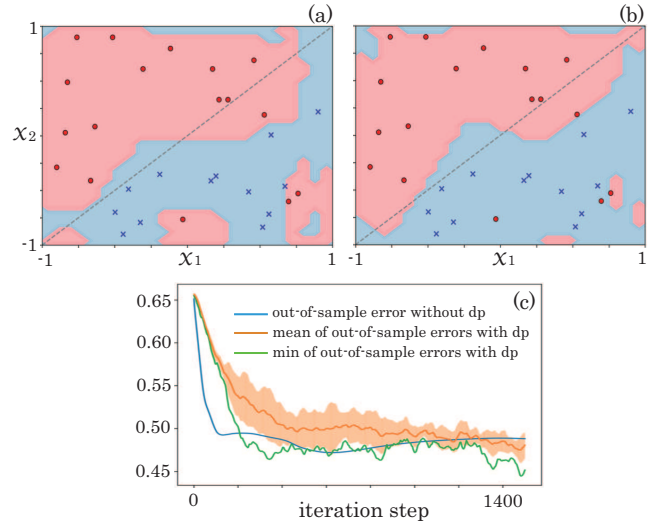


**Fig. 6** (a, b) Two-class training dataset is illustrated by the blue and red points. The constructed classifier is illustrated as the boundary dividing the blue and red regions, where (a) and (b) represent the case without dropout and with dropout, respectively. (c) Out-of-sample (test) error achieved by the classifier without dropout (blue solid line) and with dropout (mean: red solid line, min: green solid line). The orange shade represents the standard deviation of 5 learning curves, fluctuating with respect to the randomness in dropout.

### 3.3 Performance dependence on the dropout rate

In this section, we study the effect of changing the layer and gate dropout rate, for the same regression problem in Section 2.2 and 3.2; that is, both the training and test datasets are generated from  $y = \sin(\pi x)$  with Gaussian noise, and the circuit of  $n = 5$  qubits and  $L = 10$  layers is employed.

Figure 7 (a) and (b) show the in-sample error and the out-of-sample error, respectively, where the layer dropout rate is changed from 0.0 to 1.0 while the gate dropout rate is fixed to 0.3; the blue solid line shows the mean of errors over 5 sample trajectories, and the orange line is the minimum envelope of these trajectories. Because increase of dropout rate means decrease of expressibility of the approximator, the increasing trend of the in-sample error in the figure (a) makes sense. Notably, the out-of-sample takes the minimum when the layer dropout rate is 0.2; that is, if the circuit expressibility is too strong (i.e., the layer dropout rate is near 0), it overfits to the training data, and consequently the out-of-sample error becomes worse; also if the circuit expressibility is weak (i.e., the layer dropout rate is bigger than 0.3), it underfits to the training data, and the same performance degradation is observed.

To see the possibility of further decreasing the out-of-sample error, we turn to examine the case where the gate dropout rate changes from 0.0 to 1.0 while the layer dropout rate is fixed to 0.2. Figure 7 (c) and (d) show the in-sample error and the out-of-sample error, respectively (the meaning of blue and orange lines are the same as the case of (a, b)). The result is that, as shown in the figure (d), the gate dropout rate of 0.8 is the best choice in this case.

Hence, naively, the combination of small layer dropout rate and large gate dropout rate may lead to a good out-of-sample performance. This simple guide is supported by another case-study comparing two pairs of dropout rate shown in Table 1. The point of this choice is that the average number of removed CNOT gates is almost the same in these two cases. Actually, the combination of small layer dropout rate (0.2) and large gate dropout rate (1.0) yields a better performance in the out-of-sample error, compared to the opposite combination of large layer dropout rate (0.6) and small gate dropout rate (0.3). Hence lessons learned here is that the entangling dropout should be executed with care in choosing the place as well as the average number of entangling gate to be removed.

**Table 1** Comparison of two patterns of dropout (dp) rate

layer dp rate	gate dp rate	average # of removed CNOT	accuracy for training data	accuracy for test data
0.2	1.0	24	0.052	0.11
0.6	0.3	21.6	0.35	0.40

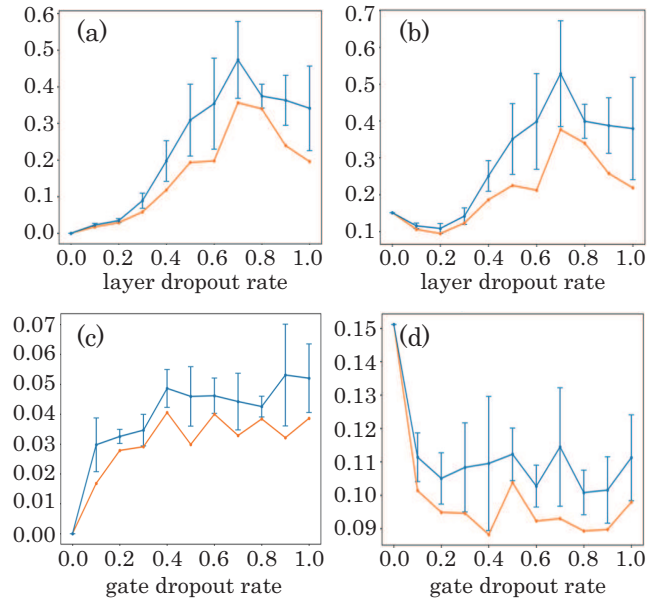


**Fig. 7** The in-sample error (a) and the out-of-sample error (b) as a function of the layer dropout rate, where the gate dropout rate is fixed to 0.3. Also the in-sample error (c) and the out-of-sample error (d) as a function of the gate dropout rate, where the layer dropout rate is fixed to 0.2. In the four figures, the blue solid line shows the mean of errors over 5 sample trajectories, and the orange line is the minimum envelope of these trajectories.

### 3.4 Comparison to $L_1$ and $L_2$ regularization

Lastly we conduct a comparison to another regularization method, i.e.,  $L_1$  and  $L_2$  regularization, which is also often used in conventional machine learning to suppress the overfitting issue. This technique is realized by simply modifying the cost function as follows:

$$J(\theta) \rightarrow J(\theta) + \lambda \sum_i |\theta_i|^p,$$

where the second term represents the penalty on freely choosing the parameters. The hyper parameter  $\lambda$  is chosen to determine the weight of this penalty.  $L_1$  and  $L_2$  regularization correspond to  $p = 1$  and  $p = 2$ , respectively. It is well known that, with this regularization, the parameters tend to have small value or become exactly zero, which thus reduce the number of effective parameters or equivalently the power of expressibility.

Here we again consider the same regression problem in Section 2.2 and 3.2, where the dataset is generated from  $y = \sin(\pi x)$  with Gaussian noise and the circuit of  $n = 5$  and  $L = 10$  is chosen as the approximator. The result is summarized in Fig. 4; in particular the approximator with and without dropout reaches the out-of-sample error of about 0.1511 and 0.1092, respectively, after 1000 parameters update.

The comparable performance can actually be achieved via the  $L_1$  and  $L_2$  methods, by carefully choosing the weighting parameter  $\lambda$ . The result is listed in Table 2; actually they

reach the value of out-of-sample error 0.1339 and 0.1483, which are smaller than 0.1511, yet are not smaller than 0.1092. Importantly, in this case  $L_1$  and  $L_2$  need 10000 steps of iteration, which is much bigger than the necessary number when using the entangling dropout.

**Table 2** Comparison of the entangling dropout and the  $L_1$  or  $L_2$  regularization method

pattern	accuracy for test data	number of iterations
without dropout	0.1511	1000
with dropout	0.1092	1000
$L_1$	0.1339	10000
$L_2$	0.1483	10000

It should be also worth studying the values of optimized parameters. Figure 8 shows those values, where the horizontal axis corresponds to the index of parameters. Interestingly, the optimized parameters obtained via the dropout method take the values (orange points) near the values without regularization (blue points); that is, the dropout method makes a slight change of parameters yet to have a large impact on the resultant out-of-sample error. This makes sense, because the dropout reduces the expressibility by directly limiting the flow of quantum information in the circuit, without largely changing the parameters of circuit. On the other hand, the  $L_1$  and  $L_2$  regularization keep the same reachable set in the original Hilbert space, and thus it carefully has to choose the parameters, which may explain the reason why 10000 iterations is necessary to learn the parameters.

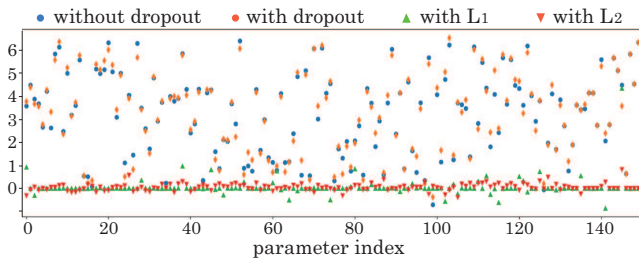


**Fig. 8** The optimized parameters for the case of  $L_1$ ,  $L_2$ , and with/without entangling dropout. The vertical axis represents the value of parameters.

## 4 Conclusion

In this paper, we proposed the entangling dropout method, for suppressing the overfitting issue in quantum machine learning problems. Some numerical demonstrations show that this method effectively achieves the goal, by directly reducing the power of entanglement and thereby limiting the reachable set in the feature Hilbert space. In general, designing an affective ansatz in quantum variational algorithms is

not an easy task; in this sense the entangling dropout can be interpreted as a method for randomly searching a proper ansatz suitable for quantum machine learning problems.

The demonstrations shown in this paper are based on only a few small-size examples, and thus we cannot draw a general perspective on the entangling dropout method. Note that it is not so important to perform various such small-size case studies. Rather, the effectiveness of the entangling dropout method should be judged in future large-size quantum machine learning settings where hopefully some quantum advantages would be established. Yet we believe it is worth sharing the idea of entangling dropout in the community, in advance to such demonstration.

**Acknowledgements** This work was supported by MEXT Quantum Leap Flagship Program Grants No. JPMXS0118067285 and No. JPMXS0120319794, and also Grant-in-Aid for JSPS Research Fellow Grant No. 22J01501.

## References

1. J. Biamonte, P. Wittek, P. Nicola, P. Rebentrost, N. Wiebe, and S. Lloyd, Quantum machine learning, *Nature* **549**, 195 (2017).
2. K. Mitarai, M. Negoro, M. Kitagawa, and K. Fujii, Quantum circuit learning, *Phys. Rev. A* **98**, 032309 (2018).
3. Havlíček, V., Córcoles, A.D., Temme, K., Harrow, A.W., Kandala, A., Chow, J.M., Gambetta, J.M.: Supervised learning with quantum-enhanced feature spaces. *Nature* **567** (7747), 209 (2019).
4. F. J. Gil Vidal and D. O. Theis, Input redundancy for parameterized quantum circuits, *Front. Phys.* **8**, 297 (2020).
5. A. P. Salinas, A. Cervera-Lierta, E. Gil-Fuster, and J. I. Latorre, Data re-uploading for a universal quantum classifier, *Quantum* **4**, 226 (2020).
6. M. Schuld, R. Sweke, and J. J. Meyer, Effect of data encoding on the expressive power of variational quantum-machine-learning models, *Phys. Rev. A* **103**, 032430 (2021).
7. M. C. Caro, E. Gil-Fuster, J. J. Meyer, J. Eisert, and R. Sweke, Encoding-dependent generalization bounds for parametrized quantum circuits, *Quantum* **5**, 582 (2021).
8. C. Gyurik, D. van Vreumingen, and V. Dunjko, Structural risk minimization for quantum linear classifiers, arXiv:2105.05566
9. L. Banchi, J. Pereira, and S. Pirandola Generalization in quantum machine learning: A quantum information standpoint, *PRX Quantum* **2**, 040321 (2021).
10. C-C. Chen, M. Watabe, K. Shiba, M. Sogabe, K. Sakamoto, and T. Sogabe, On the expressibility and overfitting of quantum circuit learning, *ACM Trans. Quantum Computing* **2**, 2, 1/24 (2021).
11. Y. Du, M-H. Hsieh, T. Liu, S. You, and D. Tao, Learnability of quantum neural networks, *PRX Quantum* **2**, 040337 (2021).
12. M. C. Caro, H-Y. Huang, M. Cerezo, K. Sharma, A. Sornborger, L. Cincio, and P. J. Coles, Generalization in quantum machine learning from few training data, arXiv:2111.05292
13. N. Srivastava, G. Hinton, A. Krizhevsky, I. Sutskever, and R. Salakhutdinov, Dropout: a simple way to prevent neural networks from overfitting, *Journal of Machine Learning Research* **15**, 1, 1929/1958 (2014).
14. G. Verdon, J. Pye, and M. Broughton, A universal training algorithm for quantum deep learning, arXiv:1806.09729
15. M. Schuld, A. Bocharov, K. M. Svore, and N. Wiebe, Circuit-centric quantum classifiers, *Phys. Rev. A* **101**, 032308 (2020).